DE GRUYTER OPEN

GEOCHRONOMETRIA 44 (2017): 66–76
DOI 10.1515/geochr-2015-0058

Available online at
http://www.degruyter.com/view/j/geochr

TESTING THE SUITABILITY OF DIM SEDIMENTARY QUARTZ FROM NORTHERN SWITZERLAND FOR OSL BURIAL DOSE ESTIMATION

MAREIKE TRAUERSTEIN[1], SALLY E. LOWICK[2], FRANK PREUSSER[3] and HEINZ VEIT[1]
[1]*Institute of Geography, University of Berne, Hallerstrasse 12, 3012 Bern, Switzerland*
[2]*Institute of Geological Sciences and the Oeschger Centre for Climate Research, University of Bern, Baltzerstrasse 1+3, 3012 Bern, Switzerland*
[3]*Institute of Earth and Environmental Sciences, University of Freiburg, Albertstraße 23b, 79104 Freiburg, Germany*

Received 22 September 2016 Accepted 20 February 2017

Abstract: We investigate the suitability of sedimentary quartz associated with former glacial advances in northern Switzerland to provide reliable burial dose estimates using Optically Stimulated Luminescence (OSL). Previous studies on northern alpine quartz show that its signal characteristics can be poor and potentially problematic. We analyse quartz signals of small aliquots, which reveal the presence of a prominent medium or slow component in the initial part of some signals. Nonetheless, rejection of aliquots with unfavourable signal composition does not alter the burial dose estimates, but significantly reduces the data set for D_e determination. Signal lifetimes from isothermal decay measurements cover a wide range of values, yet the lowest lifetimes are high enough to guarantee a reliable burial dose estimate for samples of < 400 ka. Comparison of small aliquot and single grain burial dose distributions reveals that signal averaging masks partial bleaching in some of the samples. We therefore strongly recommend single grain measurements for samples from this setting and area, in order to exclude age overestimation due to partial bleaching.

Keywords: OSL, quartz, dim, signal components, lifetime, Alps.

1. INTRODUCTION

Optically stimulated luminescence (OSL) dating of sediments associated with glacial advances in formerly glaciated areas is of importance for many palaeoenvironmental studies. One obvious scope is to reconstruct the timing and extent of glacial advances and by this contribute to the reconstruction of the regional palaeoclimate. Another valuable scope is to relate the sediment age to pedogenesis, as glacial advances provide fresh parent material for soil formation. The former Rhone-Aare-glacier in northern Switzerland is considered a key location for investigating pedogenesis in relation to sediment age, but a robust chronology for the sediments is still needed. A major potential problem in the dating of sediments from glacial environments results from potential incomplete bleaching of the OSL signal prior to deposition (Spencer and Owen, 2004; Duller, 2006; Preusser *et al.*, 2007), which will lead to overestimation of the burial age if not detected and corrected for. As quartz is more readily bleachable than feldspar (Godfrey-Smith *et al.*, 1988; Murray *et al.*, 2012), it is the preferred mineral for such sediments. Furthermore, OSL measurements at a single grain scale have proven to be a powerful tool in assessing if a deposit suffers from partial bleaching (e.g. Olley *et al.*, 2004; Duller, 2006). Here, the methodology is far more advanced and better understood for quartz in comparison to feldspar. However, several studies dealing with OSL dating of alpine quartz have reported problems

Corresponding author: M. Trauerstein
e-mail: mareike.trauerstein@giub.unibe.ch

ISSN 1897-1695 (online), 1733-8387 (print)

with low signal intensities (Klasen *et al.*, 2007, 2016; Preusser *et al.*, 2007; Bickel *et al.*, 2015; Lowick *et al.*, 2015; Rades *et al.*, in press). This phenomenon appears to be common for sediments originating from geologically young orogenies and might be explained by the lack of natural signal sensitisation through multiple cycles of bleaching and dosing prior to deposition (Moska and Murray, 2006; Preusser *et al.*, 2006; Pietsch *et al.*, 2008). While some studies point out additional problems with dating northern alpine quartz due to unstable signal components (Klasen, 2008; Klasen *et al.*, 2016; Bickel *et al.*, 2015), other studies do not observe such problems (Gaar *et al.*, 2014; Salcher *et al.*, 2015; Schielein *et al.*, 2015). This might be explained by the complex geological composition of the Alps and related differences in the origin (magmatic versus metamorphic) and history of quartz grains in different regions. For example, quartz derived from sedimentary rocks may have undergone several depositional cycles in the past. Hence, it is crucial to test each catchment individually and this study aims to carefully assess the suitability of quartz from the area of the former Rhone-Aare-glacier.

In order to appropriately address potential problems with signal composition, small aliquot measurements were carried out, as their signals can be properly analysed in respect to the component composition. This analysis of the component composition is considerably more complicated for single grain signals, as the signal decay might rather reflect the degree of laser-grain coupling than true decay rate (Thomsen *et al.*, 2012; 2015). Together with standard tests (preheat dose recovery tests, dose recovery test) of the Single Aliquot Regenerative Dose (SAR protocol), signal component analysis was conducted using mathematical deconvolution (McKeever and Chen, 1997; Bulur, 2000), and fast ratios were determined (Durcan and Duller, 2011). The effect of the signal composition was investigated by using the fast ratio as a rejection criterion in different ways and by choosing different background integral intervals (early background approach, Ballarini *et al.*, 2007; Cunningham and Wallinga, 2010). Even though the small aliquot signals were dim and are likely to originate from only a small fraction (<10%) of all quartz grains (e.g. Duller *et al.* 2000), additionally, single grain analyses were carried out in order to check if the samples are affected by partial bleaching, that could not be detected in the small aliquot datasets.

2. MATERIALS AND METHODS

The study was performed on nine samples chosen from a set of ~40 samples that were collected from the research area. Seven samples originate from deposits that are associated with the last glacial advance of the Rhone-Aare-glacier on the Swiss Plateau (outwash deposits), and two samples are taken from deposits formed by periglacial processes such as slope wash and solifluidal transport (Table S1, supplementary material). The sediments originate from bedrock in the source areas of the Rhone-Aare glacier, which comprise a large variety of rock types, including plutonic (granitic) basement and metamorphic rocks of the core of the Alps, carbonates and clastic sediments of the Prealps (Helveticum), and sandstones of the Molasse Basin. As the latter represent debris eroded during the main orogenesis, the origin of grains will also be complex.

Samples were collected by inserting stainless steel tubes into the vertically exposed sediments. They were prepared under subdued red light to avoid depletion of the natural OSL signal. For equivalent dose (D_e) determination, samples were dry sieved to separate the 150–200 µm grain size fraction, followed by HCl and H_2O_2 treatment to remove carbonates and organics, respectively. A quartz and potassium-rich feldspar fraction was extracted using heavy liquids (2.70 g cm^{-3}, 2.58 g cm^{-3}), and the quartz was subsequently etched in 40% HF for 1 h. The etched quartz was treated with 30% HCl for 1 h to eliminate any acid-soluble fluoride precipitates, and sieved again to remove disaggregated quartz grains and partially etched feldspars. For small aliquot measurements, grains were dispensed onto stainless steel discs in diameters of 2 mm (~150 ± 50 grains). For single grain measurements, the grains were mounted on aluminium discs that hold 100 grains each in 300 mm diameter holes (Bøtter-Jensen *et al.*, 2003).

Luminescence measurements were carried out on a Risø DA-20 TL/OSL single grain reader fitted with an internal $^{90}Sr/^{90}Y$ beta-source. To account for possible spatial non-uniformity of the dose rate each position on the single grain disc was individually calibrated (Thomsen *et al.*, 2005; Ballarini *et al.*, 2006). Small aliquots were stimulated with blue (470 ± 30 nm) light emitting diodes (LEDs), single-grain OSL signals were stimulated using a green (532 nm) laser. Ultraviolet (UV) emissions were detected through a 7-mm-thick and 2.5-mm-thick Hoya U-340 filter for small aliquot and single grain measurements, respectively.

Equivalent dose (D_e) estimates were obtained using the SAR protocol described in Murray and Wintle (2000), complemented with an additional step to check for feldspar grains or inclusions (IR depletion ratio, Duller, 2003), and modified for the single grains by using stimulation with an IR laser. In order to evaluate the ability of the SAR-protocol to recover a known laboratory dose, a number of dose recovery tests were conducted on sample material previously exposed to a Sunlux Ambience UV lamp for 24 h. To identify any dependence of the recovered dose on temperature (Wintle and Murray, 2006), preheat dose recovery tests were conducted for large aliquots (6 mm) of sample STH01 and ABH09. The tests were performed at temperatures between 210 and 290°C, using four aliquots per temperature step (given dose ~80 Gy, test dose ~20 Gy). In order to further test the protocol and determine the spread of the recovered doses, dose recovery tests were carried out on 48 aliquots of

sample ABH08 and RUM04 (given dose ~50 Gy and ~60 Gy respectively, test dose ~20 Gy). D_e values for small aliquots were determined using a single saturating exponential fit for the dose response curve and an instrument error of 1.5%. The measured signal was integrated over the first 0.4 s. Aliquots were accepted if they had a natural signal more than 3 sigma above background, a test dose error < 15%, a recuperation signal (as % of highest given dose) < 5%, a recycling ratio that did not deviate more than 10% from unity within errors and an IR depletion ratio > 0.8.

For single grains, dose recovery tests were performed on four samples (ABH07, ABH07, AM01, and DM02). D_e was determined using a single saturating exponential fit for the dose response curve, an instrument error of 2.5% and the signal was integrated over the first 0.05 s. Grains were accepted if they had a test dose error < 15%, a recuperation signal (as % of highest given dose) < 5%, a recycling ratio not deviating more than 10% from unity within errors and an IR depletion ratio > 0.6. We chose this lower IR depletion ratio threshold for the single grain measurements than for the small aliquot measurements as, for most samples, there is a clear gap in IR depletion ratios between ~0.4 and 0.6 – making it straightforward to distinguish between pure quartz and feldspar grains/grains with feldspar inclusions (Fig. S1, supplementary material).

It has been shown that the quartz OSL signal consists of a number of discrete components (Smith and Rhodes, 1994; Bailey *et al.*, 1997; Jain *et al.*, 2003), which are characterized by unique thermal and optical properties. In order to quickly assess the component composition of the signals, we determined the fast ratio (Durcan and Duller, 2011). The fast ratio compares the intensity of the initial signal on an OSL decay curve, which should be dominated by the fast component, with an integral further along the decay curve chosen to represent the contribution of the medium component (Durcan and Duller, 2011). The fast ratio was calculated for the natural and the regenerated signal (measured after giving the second laboratory dose of the SAR protocol) of each aliquot. Durcan and Duller (2011) recommend the use of signal from the first channel to represent the fast ratio, because the relative contribution from the fast component to the total signal at this point will be at a maximum. We chose to increase this integral to 0.4 s, which is also the integral used for D_e determination in this study, as our signals are very dim and this reduces the associated error due to counting statistics. Although this lowers the fast ratio values, the precision is improved and the relative differences between the signals become more meaningful.

3. RESULTS AND DISCUSSION

Performance tests and D_e determination

Fig. 1 shows the results of the preheat dose recovery test using large aliquots. There appears to be no relationship between preheat temperature and recovered dose, but recovery ratios are generally low for sample ABH09 (around 0.9). This is why, for the following dose recovery tests on small aliquots and single grains, a preheat of 250°C for 10 s was chosen. The results of the small aliquot dose recovery tests reveal, similar to the preheat dose recovery test, that the recovered dose of one sample (ABH08) slightly underestimates the given dose. The recovered dose distribution of this sample is characterized by an overdispersion (OD) of 18%, whereas for the second sample (RUM04) the given dose is recovered within errors and no OD is observed. This differences in OD may be due to different intrinsic characteristics of the samples. For single grains, recovered doses are 0.90 ± 0.03 (ABH07), 0.89 ± 0.05 (ABH08), 1.10 ± 0.04 (AM01) and 0.91 ± 0.05 (DM02) with OD values ranging between 11 and 23%.

Of the measured small aliquots for D_e determination, about half of them do not pass the acceptance criteria (see **Table 1**). Between 0 and 31% of the measured aliquots do not exhibit a natural signal more than 3 sigma above background and/or a test dose error < 15%, additionally, between 17 and 54% do not pass the recycling ratio and/or IR depletion ratio acceptance criterion. Small aliquot signals usually do not approach saturation (they do not exceed $2D_0$).

Of the measured single grains, only a very small percentage (between 0.6 and 3.2%, depending on the sample) is accepted for D_e determination. Between 94.0 and

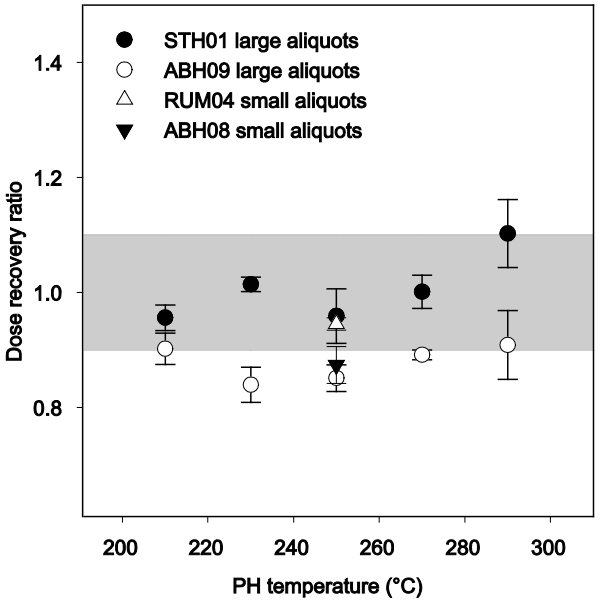

Fig. 1. *Results of the preheat dose recovery tests (large aliquots) for sample STH01 and ABH09 and the small aliquot dose recovery tests for sample RUM04 and ABH08. Large aliquot dose recovery ratios were calculated using the arithmetic mean with standard error, small aliquot dose recovery ratios were calculated using the Central Age Model (CAM).*

Table 1. *Small aliquot data. N = number of aliquots measured, n = number of aliquots used for D_e calculation, OD = overdispersion, D_e - CAM = equivalent dose calculated using the Central age model by Galbraith et al. (1999), A = to select aliquots for D_e calculation conventional rejection criteria were applied as described in chapter 2, B = individuals D_es were determined using an early background and conventional rejection criteria were applied, C = conventional rejection criteria were applied and additionally all aliquots with $FR_{nat} \neq FR_{reg}$ were excluded, D = conventional rejection criteria were applied and additionally all aliquots with FR_{nat} and $FR_{reg} < 15$ were excluded.*

		A: Conventional approach			B: EBG approach			C: $FR_{nat} = FR_{reg}$ approach			D: FR > 15 approach		
	N	n	OD (%) /skew	D_e - CAM (Gy)	n	OD (%)	D_e - CAM (Gy)	n	OD (%)	D_e - CAM (Gy)	n	OD (%)	D_e - CAM (Gy)
ABH07	48	22	33/0.35	74.8 ± 5.4	27	35	80.1 ± 5.7	11	29	78.9 ± 7.1	3	37	86.6 ± 18.8
ABH08	45	32	27/0.11	105.9 ± 5.3	28	25	111.2 ± 5.6	16	23	99.4 ± 6.2	14	28	115.7 ± 8.9
ABH09	48	26	36/0.69	103.8 ± 7.6	21	36	113.9 ± 9.6	14	27	92.5 ± 7.3	7	42	109.5 ± 17.7
STH01	45	24	29/–0.40	156.5 ± 9.8	25	31	172.4 ± 11.6	6	38	144.9 ± 23.5	6	25	156.6 ± 16.7
IFF01	28	13	56/0.55	113.7 ± 11.9	13	61	112.2 ± 19.2	4	24	118.7 ± 14.7	7	56	128.3 ± 27.1
RUM04	45	24	30/0.68	70.8 ± 4.8	13	26	75.6 ± 5.9	13	26	64.7 ± 5.1	2	-	84.9 ± 3.3
ATH01	86	32	39/0.17	104.9 ± 7.6	33	38	107.1 ± 7.6	16	40	108.0 ± 8.9	9	51	98.9 ± 17.1
ATH04	72	17	38/–0.75	52.9 ± 5.2	13	25	65.4 ± 5.2	9	44	49.4 ± 7.7	8	26	64.6 ± 6.2
DM02	41	22	27/-0.79	16.1 ± 1	19	28	15.9 ± 1.2	19	27	15.7 ± 1.1	2	-	12.8 ± 3.1

98.9% of the grains are rejected because they do not exhibit a natural signal more than 3 sigma above background and/or a test dose error < 15%. A smaller percentage (between 0.3 and 3.6%) are additionally rejected, because they do not meet the recuperation, recycling and/or IR depletion ratio criterion. At last, between 0 and 0.3% of the grains are additionally rejected because their D_e values were above $2D_0$ or oversaturated. For all samples the D_e values were routinely plotted against signal intensity but no relationship is observed.

Signal composition of small aliquot signals

Fig. 2 shows the component composition for an aliquot signal with a high and a low fast ratio assessed by mathematical deconvolution (McKeever and Chen, 1997; Bulur, 2000). The higher the fast ratio, the more the initial signal is dominated by the fast component. According to Durcan and Duller (2011), in signals with a fast ratio > 10 the fast component contributes > 80%, while in signals with a fast ratio > 20, the contribution of the fast component is > 90%.

A large number of the calculated fast ratios are relatively low (< 10), i.e. the fast component in the initial signal is less than ~80% (Durcan and Duller, 2011). For up to half of the aliquots per sample, there is a discrepancy between the fast ratios of natural and regenerated dose signals, the fast ratios do not agree within errors. **Fig. 3** shows the determined fast ratio for the natural signal plotted against the fast ratio of the regenerated signal for each aliquot of sample ATH01 and STH01. Such an observed discrepancy between the component contributions may indicate the presence of a component that is thermally unstable (Li and Li, 2006; Steffen *et al.*, 2009), has a high recuperation (Jain *et al.*, 2003), sensitised differently during the SAR protocol (Jain *et al.*, 2003), or is bleached to a different degree than the other components before burial (e.g. Bailey, 2003). These phenomena may also be a problem for aliquots where fast ratios agree within

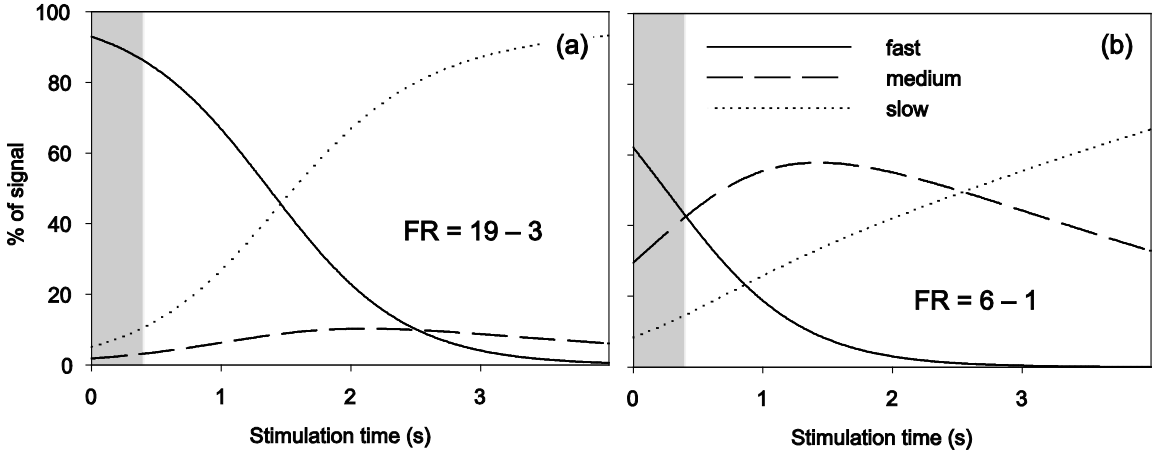

Fig. 2. *Mathematically deconvoluted signals of (a) a signal with a high fast ratio (FR = 19 ± 3) and (b) a low fast ratio (FR = 6 ± 1). Shaded area represents the time integral over which the initial signal was integrated (0.4 s).*

errors, but may not be visible due to their competing effects.

All aliquots with an IR depletion ratio <0.8 also exhibit a fast ratio <10 (**Fig. 3**, black dots). Feldspar contamination for these samples can therefore be excluded by either using the IR depletion ratio or the fast ratio as a rejection criterion, as has also been suggested by Fu *et al.* (2015). However, when using the latter criterion, aliquots with non-contaminated signals are also automatically rejected, which may be unnecessary.

Effects of signal composition on small aliquot D_e

The small aliquot D_e distributions following the conventional rejection criteria (Chapter 2) are normally distributed to slightly positively skewed (skew < 0.7) and display OD values between 27 and 39% (**Table 1**). As the signal component analysis has shown that many of the signals exhibit a rather weak fast component, its effect on the D_e determination was investigated. A dominant fast component in the OSL signal is one of the underlying assumptions when using the SAR protocol for quartz OSL dating (Wintle and Murray, 2006).

One way to explore the effect of the signal composition on D_e determination is to apply the early background (EBG) approach (Ballarini *et al.*, 2007, Cunningham and Wallinga, 2010), where the signal measured immediately following the initial portion of signal decay is used to calculate the background. This is done to minimise the influence from any medium and slow components, and leaves a net signal dominated by the fast component. We used an EBG interval immediately following the initial signal interval and 2.5 times its duration as suggested by Cunningham and Wallinga (2010). For the small aliquot signals, this represents the first 0.4 s and a background averaged over the 0.5–1.4 s interval of signal decay. Applying this approach to the small aliquot dose recovery tests slightly increases the dose recovery ratio of sample ABH08 from 0.88 ± 0.03 to 0.90 ± 0.04, although the ratios still agree within errors. For sample RUM04 the ratio slightly decreases from 0.95 ± 0.01 to 0.93 ± 0.02 and the OD increases from 0 to 7%.

Another approach to explore the effect of component composition is to introduce the fast ratio as an additional acceptance criterion and two approaches are potentially useful in this context. One possibility is to reject all aliquots with a significant discrepancy between fast ratio of the natural and the regenerated signal (values do not agree within errors). This strategy assumes that a weak fast component in the initial signal is not necessarily a problem as long as the component composition is similar in the fast and the regenerated signal (as this is a sign of their stability and similar sensitisation during the SAR protocol). Any competing effects that might average out the influences on the components are not considered in this approach. Applying this criterion to the small aliquot dose recovery test increases the dose recovery ratio of sample ABH08 from 0.88 ± 0.03 to 0.92 ± 0.03 and leaves the dose recovery ratio of sample RUM04 unchanged.

Another possibility is to set an acceptance threshold for the fast ratio that both the natural and the regenerated signal should meet. Durcan and Duller (2011) recommend the use of a fast ratio threshold of 20 to guarantee reliable dating. Other studies have used lower thresholds

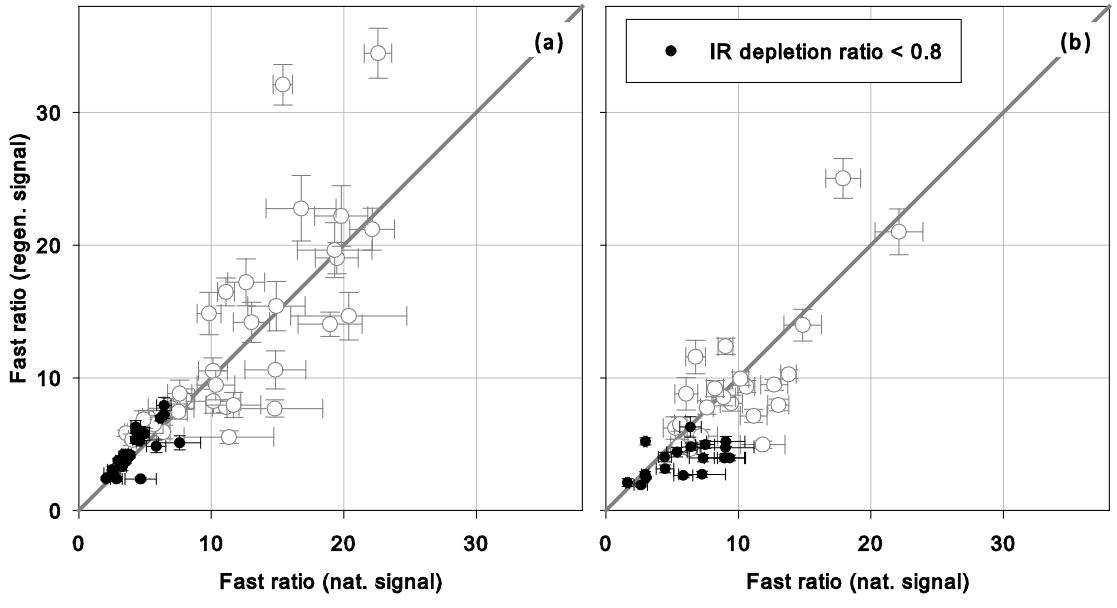

Fig. 3. *Fast ratio for the natural signal plotted against the fast ratio of the regenerated signal for each aliquot of sample ATH01 (a) and STH01 (b). White dots show aliquots with an IR depletion ratio > 0.8, black dots show aliquots with an IR depletion ratio < 0.8.*

(e.g., Fu *et al.*, 2015; Feathers, 2015) following the suggestion of Duller (2012) to analyse the average D_e as a function of fast ratio and then choose a fast ratio threshold at which the D_e outcome is stable. Feathers (2015) observes a stable D_e beyond a threshold of 2 for his single grain data, and Fu *et al.* (2015) observe a stable D_e beyond a threshold of 15 for small aliquot data but without applying the IR depletion ratio as a rejection criterion. In this study we applied different fast ratio thresholds to our dose recovery data in order to identify a fast ratio threshold that is appropriate for testing the D_e determination. The dose recovery ratio of sample RUM04 appears to be independent of the fast ratio threshold and OD (as the latter was already 0% without applying any fast ratio threshold). It should be noted, however, that applying a threshold of 15 leaves only four values. The dose recovery ratio of sample ABH08 increases slightly from 0.88 ± 0.03 to 0.92 ± 0.04 beyond a fast ratio threshold of 14. We cannot exclude that this is simply coincidental, but despite this, a fast ratio of 15 is considered appropriate for testing the effect of signal composition on D_e determination as increasing the threshold above this, reduces the number of accepted aliquots to a number that prevents a robust calculation of the D_e. A fast ratio of 15 corresponds to a fast component contribution to the initial signal of > 85% (Durcan and Duller, 2011).

Fig. 4 compares the results of D_e determination using the different approaches described above (A – conventional approach, B – EBG approach, C – fast ratio of natural and regenerated signal agree within errors, D – fast ratio of natural and regenerated signal > 15). For most samples the calculated D_es using the different approaches agree within errors, suggesting that signal composition has no significant effect on D_e determination. For those samples where the outcome differs slightly (RUM04, ATH04, DM02) there is no clear pattern (systematic increase or decrease of D_e) and may be due to a dramatically reduced dataset.

Signal stability of small aliquot signals

The results of the previous section suggest that the signal composition does not influence the outcome of D_e determination, and imply that even signals with a strong medium component are suitable for dating. It was already concluded by Bailey (2010) that the absence of a strong fast component is not necessarily problematic as the thermal stability of the signal is essential in this context. Isothermal decay measurements (Murray and Wintle, 1999) using continuous wave OSL (CW-OSL) were conducted to identify the lifetime of the signal at varying temperatures for sample ABH09 and STH01. A set of 8 small aliquots (2 mm) per sample was first used for D_e determination and then given a dose of ~100 Gy, followed by a preheat of 250°C for 10 s (as for D_e determination). Similar to the approach of Buechi *et al.* (2017), the aliquot was then held for various times, between 0 and 5000 s, at elevated temperatures of between 220

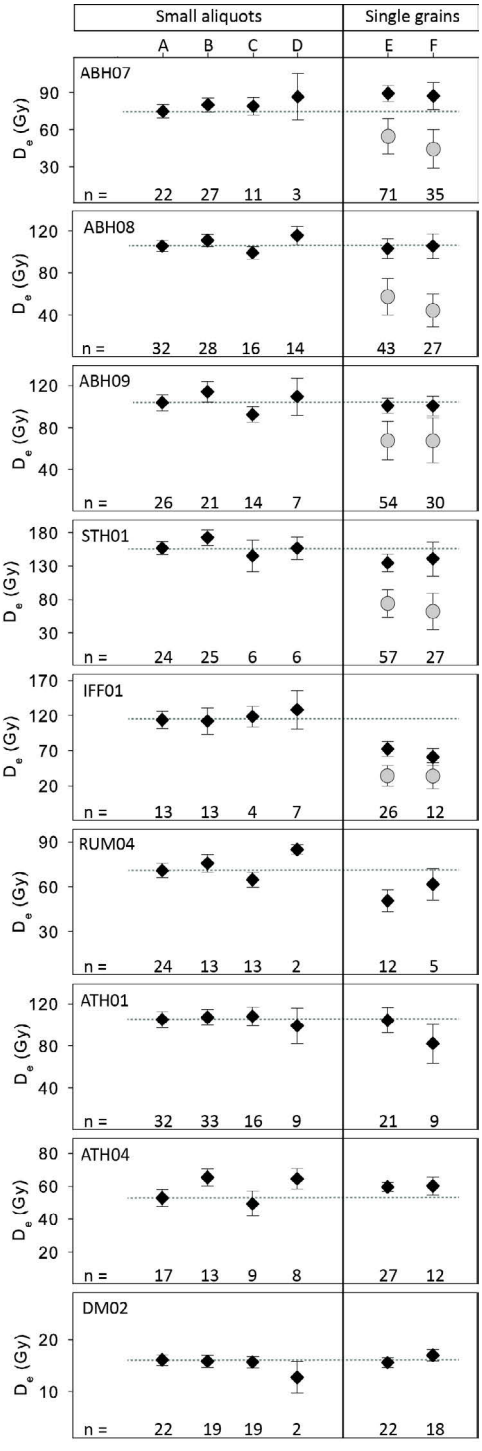

Fig. 4. *Small aliquot (A–D) and single grain (E–F) D_e values obtained with different approaches and for samples in this study. n = number of aliquots used for D_e calculation; filled symbols = D_e calculated using the Central age model (Galbraith et al., 1999); open symbols = D_e calculated using the Minimum Age Model (MAM3, sigma b = 0.3) (Galbraith et al., 1999); A – conventional rejection criteria; B – EBG approach, C – rejection of aliquots with fast ratio (natural) ≠ fast ratio (regen); D – rejection of aliquots with fast ratio (natural) and/or fast ratio (regen) < 15; E – conventional rejection criteria; F – EBG approach. Horizontal lines extending the results of approach A are added for easier comparison of values.*

and 280°C, after which the remaining signal was measured, followed by a 20 Gy test dose. For an ambient temperature of 20°C, lifetimes range between 1.1 ± 0.1 and 51 ± 1 Ma; (Fig. 5). It is not clear if this variability is due to intra-sample variability or to the measurement procedure. A lifetime of at least 20 times that of the burial age of a sample is recommended to avoid age underestimation due to loss of signal over time (Aitken, 1998), and this would suggest that already samples of > 50 ka may be affected by age underestimation. However, the present mean annual temperature on the Swiss Plateau is around 9°C and was certainly lower during most of the last 100 ka. Therefore, lifetimes at 10°C are considered more appropriate in order to evaluate if signal instability poses a problem for the samples investigated here, and would lead to a range of lifetimes between 8.2 ± 0.7 and 510 ± 10 Ma. The lowest measured lifetime at 10°C (8.2 ± 0.7 Ma) suggests that the signal should be stable for at least 400 ka, indicating that the samples of interest (expected to be younger than 100 ka) are well within the reliable dating range.

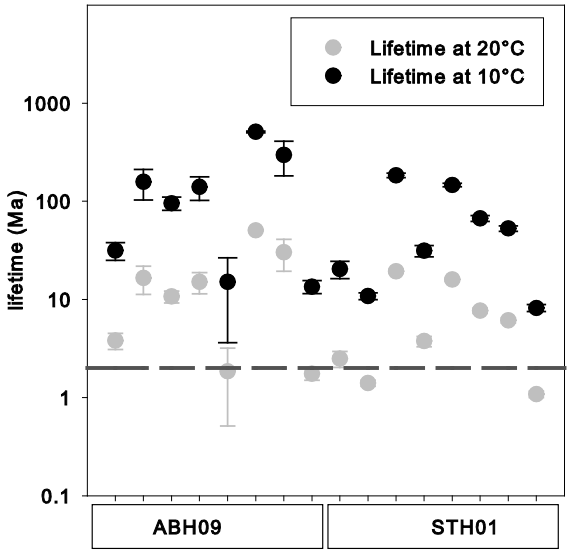

Fig. 5. *Lifetimes calculated from isothermal decay measurements for sample ABH09 and STH01 at 10 and 20°C. Dotted line indicates the lifetime required for a stable signal of samples <100 ka (expected age of samples in this study).*

Fig. 6 shows the lifetimes at 10°C plotted against the previously determined D_e values and fast ratios of the regenerated signal. There is no apparent relationship between lifetime and D_e value, in agreement with the previously reasoned assumed stability of the quartz signal. There is a very vague positive correlation between lifetime and fast ratio (R^2 = 0.43 and 0.18 for a linear regression), which may point to the influence of a thermally less stable or unstable medium component; where the medium component contributes significantly to the signal (low fast ratio), the overall signal stability is also lower.

Dose distributions

Six out of nine of the small aliquot dose distributions show a slight positive skew (skew 0.1–0.7, see Table 1) but at the same time OD values are moderate and relatively uniform (27–39%). Hence, it is difficult to decide if the samples are suffering from partial bleaching and single grain distributions were analysed to further investigate this issue.

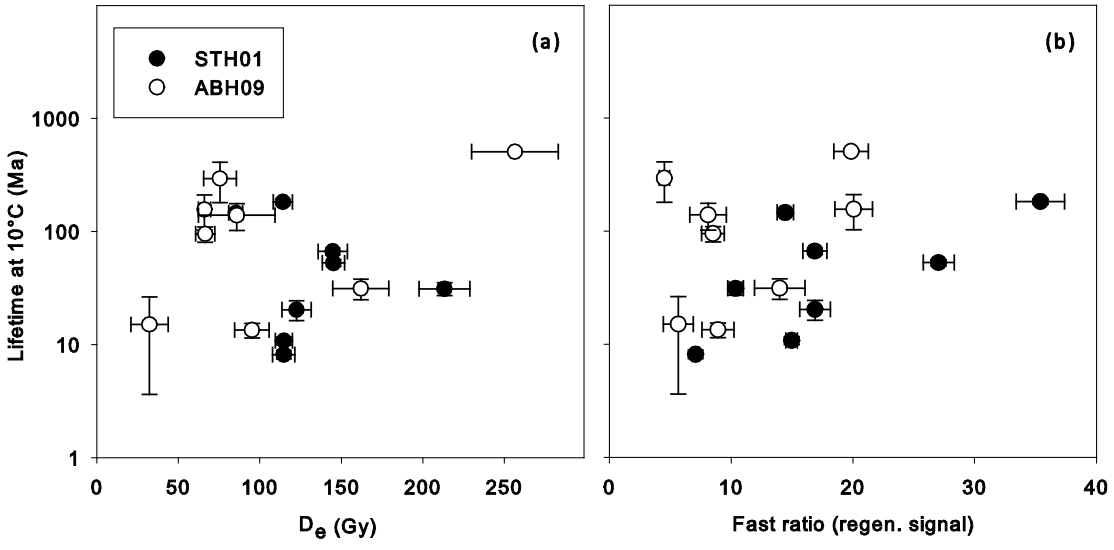

Fig. 6. *Lifetimes at 10°C plotted for each measured aliquot against (a) its previously determined D_e value and (b) fast ratio of the regenerated signal.*

Single grain measurements reveal that between 1 and 6% of the measured grains exhibit a signal more than 3 sigma above background and a test dose error < 15%. Besides, there is also a large number of dim grains that contributes to the total signal sum (Fig. S2 in the supplementary material). As one small aliquot contains 150 ± 50 grains at least part of the resulting signals will be affected by signal averaging. The single grain D_e distributions show rather large differences in shape and overdispersion, and for five of the nine samples the distributions are clearly skewed towards higher values, displaying overdispersion values of up to 74% (**Table 2**). The most likely explanation for the observed skewness combined with high overdispersion values is that samples were differentially bleached prior to deposition (Wallinga, 2002). This interpretation is supported by the fact that the samples are taken from sedimentary setting that are likely to be affected by partial bleaching (Fuchs and Owen, 2008).

The Minimum Age Model (MAM, Galbraith *et al.*, 1999) is considered appropriate for the calculation of mean D_e values for these samples. We also applied the MAM to sample STH01 although it is only slightly skewed, but with an OD of 69%. The sigma b value was chosen based on the average OD of the symmetric, and therefore likely to be "well-bleached" single grain distributions of the samples in this study. This is supported by Gaar and Preusser (2012) and Gaar *et al.* (2014), who suggest OD values of around 0.30 as input value for the MAM when analysing single grain quartz D_e distributions of samples from northern Switzerland.

Effects of signal composition on single grain D_e

Single grain measurements revealed skewed D_e distributions for five out of the nine samples which we interpret as an indication of partial bleaching. Nonetheless, it is important to also exclude the possibility that these distributions are the result of different signal composition characteristics (e.g. stable and unstable signals) instead. For the single grain signals, we considered the fast ratio and the EBG approach as possibilities to investigate the effect of signal composition on single grain D_e. The EBG approach was applied using the initial signal interval of the first 0.05 s and a background averaged over the 0.06–0.18 s interval of the signal. The fast ratio has been used in several single grain studies (e.g., Duller, 2012; Jacobs *et al.*, 2013; Feathers, 2015), although its significance is considered problematic due to the uncertain power delivery of the green laser (Thomsen *et al.*, 2012, 2015). In order to determine the fast ratio of the natural single grain signals of our samples, we chose the first 0.02 s to represent the fast component and the average signal over the 0.18–0.22 s interval to represent the medium component, following Feathers (2015) and Jacobs *et al.* (2013) who both use these intervals for 90% laser power. Given the afore mentioned difficulties, these integrals can only be considered approximate (Feathers, 2015). Due to the relatively dim signals, we encountered problems with large uncertainties, as well as negative and inflated values (cf. Durcan, 2012).

Fig. 7 shows the dependence of the single grain dose recovery ratios on fast ratio threshold and EBG approach, respectively. There is no obvious systematic dependence on fast ratio threshold nor on EBG approach. In **Fig. 8** the single grain D_e distribution of sample ABH07 is displayed with filled symbols showing grains with natural signals that exhibit a fast ratio >20. There seems to be no significant change to the distribution by only using grains with fast ratios >20. As the calculation of the fast ratio for single grain signals leads to large uncertainties, and no clear effect in applying a fast ratio threshold is observed for the dose recovery ratios nor the D_e distributions, we decided to use only the conventional and EBG approach to calculate CAM and MAM doses for our single grain data (**Fig. 5**, **Table 2**). While the CAM doses using the conventional and EBG approach agree well, there is a tendency towards slightly younger MAM ages when applying the EBG approach. We assume that this may be

Table 2. *Single grain data. N = number of grains measured, n = number of grains used for D_e calculation, OD = overdispersion, Skew of D_e distribution following Bailey and Arnold (2006), D_e - CAM = equivalent dose calculated using the Central age model by Galbraith et al. (1999), E = to select aliquots for D_e calculation conventional rejection criteria were applied as described in chapter 2, F = individuals D_es were determined using an early background and conventional rejection criteria were applied.*

	N	E: Conventional approach					F: EBG approach				
		n	OD (%)	Skew	D_e - CAM (Gy)	D_e - MAM (Gy)	n	OD (%)	Skew	D_e - CAM (Gy)	D_e - MAM (Gy)
ABH07	2200	71	58	1.15	89.3 ± 6.5	54.8 ± 7.8	35	73	0.72	87.2 ± 11	44.4 ± 15.5
ABH08	2400	43	56	0.79	103.4 ± 9.2	57.4 ± 17.1	27	54	0.32	105.9 ± 11.5	62.8 ± 23.2
ABH09	2900	54	49	1.19	100.9 ± 7.2	67.7 ± 18.3	30	48	0.52	100.8 ± 9.4	67.9 ± 21.5
STH01	5700	57	69	0.24	134.6 ± 12.8	74.1 ± 20.6	27	92	–0.08	140.7 ± 25.5	62.1 ± 27.2
IFF01	3100	26	74	1.36	72.4 ± 10.8	34.1 ± 14.5	12	69	1.27	61.1 ± 12.5	34.5 ± 18.6
RUM04	2000	12	48	–0.35	50.6 ± 7.4	-	5	34	0.01	61.6 ± 10.6	-
ATH01	3000	21	36	–0.28	104.3 ± 12.1	-	9	65	0.02	82.1 ± 18.5	-
ATH04	3000	27	19	–0.77	59.6 ± 2.8	-	12	26	–1.21	60.2 ± 5.4	-
DM02	1400	22	24	–0.74	15.6 ± 0.9	-	18	24	0.51	16.9 ± 1.1	-

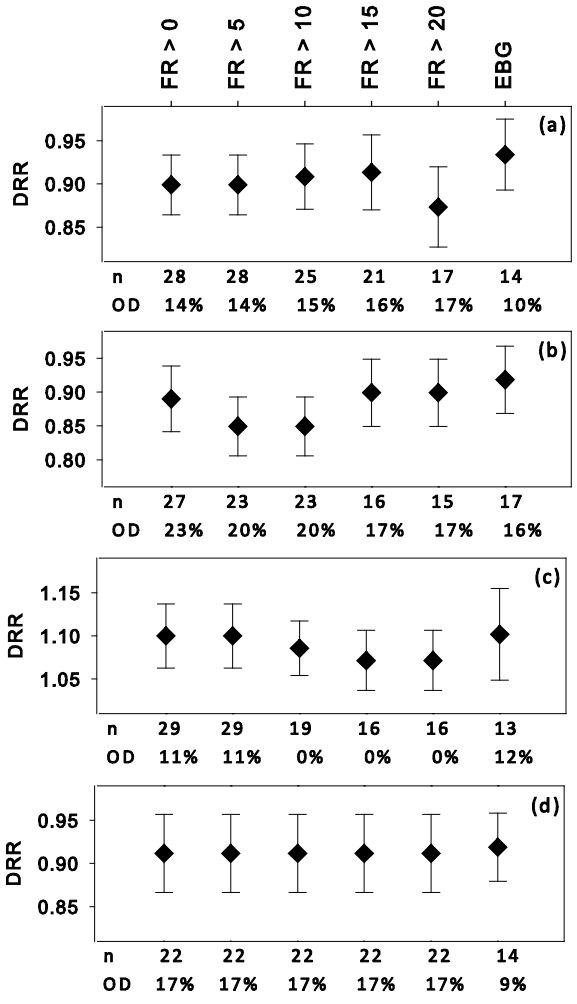

Fig. 7. *Single grain dose recovery ratios (DRR), number of grains (n) and overdispersion (OD) for different fast ratio thresholds (FR) and the EBG approach for sample ABH07 (a), ABH08 (b), AM01 (c) and DM02 (d).*

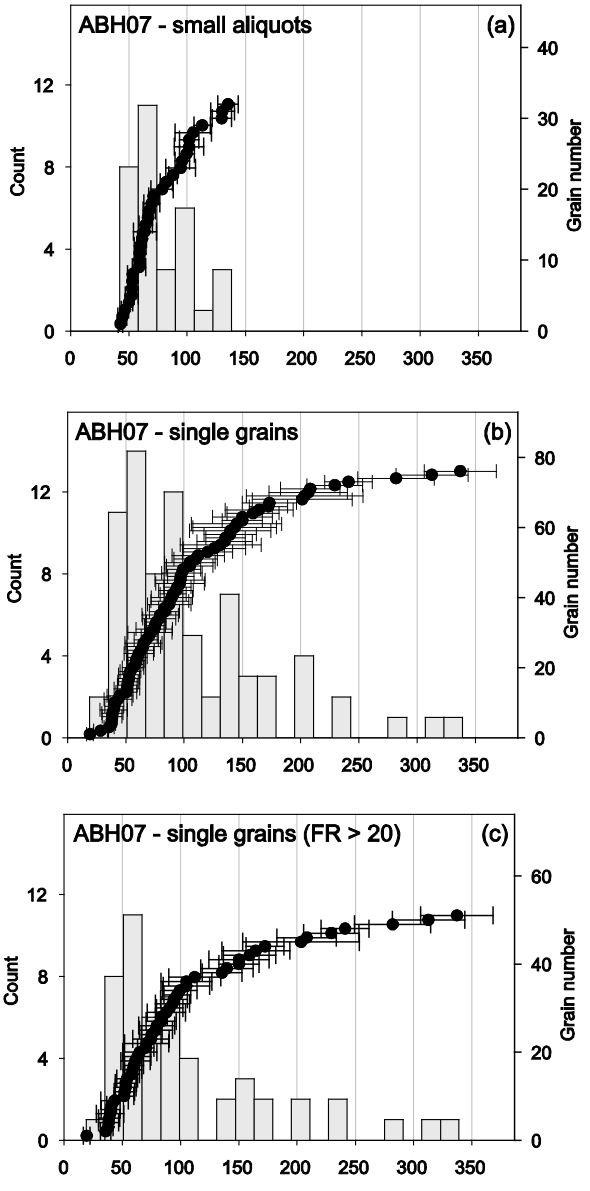

Fig. 8. *Single grain D_e values plotted as histogram (bin width = 16) and individual values in ranked order for sample ABH07. Bin with of Filled symbols show grains with natural signals that exhibit a fast ratio > 20.*

explained by the reduced dataset. Despite this, the resulting MAM doses of both approaches agree within errors, and there is therefore no obvious reason to support the EBG approach over the conventional one for the samples of this study.

4. CONCLUSIONS

A considerable number of the small aliquot quartz signals from the nine samples investigated in this study exhibit a weak fast component. Fast ratio analyses reveal that for a notable number of aliquots the signal composition between natural and regenerated signals differs significantly. Investigating the effects of signal composition on D_e shows that the latter is not dependent on whether these aliquots are excluded or not. Isothermal decay measurements confirmed that the small aliquot quartz signals are thermally stable over at least 400 ka at 10°C.

The analysis of single grain quartz data reveals that signal averaging can be present even in the very dim small aliquot signals and some samples suffer from partial bleaching. Fast ratio analyses of the single grain signals – which can only be considered approximate – support our interpretation that the skewed single grain distributions are actually the result of partial bleaching and not of differences in signal composition of the single grain signals. We therefore recommend to investigate these samples on a single grain level to detect potential partial bleaching. Ideally, evidence of partial bleaching shown by skewed D_e distributions should be backed up by comparison to feldspar dating.

ACKNOWLEDGEMENTS

MT was financially supported by Swiss National Science Foundation grant No. 149124. SEL was partly funded through the National Cooperative for the Disposal of Radioactive Waste (Nagra), Switzerland.

REFERENCES

Aitken, M. J., 1998. An Introduction to Optical Dating. 279 pp. Oxford University Press, Oxford.

Bailey RM and Arnold LJ, 2006. Statistical modelling of single grain quartz De distributions and an assessment of procedures for estimating burial dose. *Quaternary Science Reviews* 25(19–20): 2475–2502, DOI 10.1016/j.quascirev.2005.09.012.

Bailey RM, Smith BW and Rhodes EJ, 1997. Partial bleaching and the decay form characteristics of quartz OSL. *Radiation Measurements* 27: 123–136, DOI 10.1016/S1350-4487(96)00157-6.

Bailey RM, 2003. Paper I: the use of measurement-time dependent single-aliquot equivalent-dose estimates from quartz in the identification of incomplete signal resetting. *Radiation Measurements* 37: 673–683, DOI 10.1016/S1350-4487(03)00078-7.

Bailey RM, 2010. Direct measurement of the fast component of quartz optically stimulated luminescence and implications for the accuracy of optical dating. *Quaternary Geochronology* 5: 559–568, DOI 10.1016/j.quageo.2009.10.003.

Ballarini M, Wallinga J, Wintle AG and Bos AJJ, 2007. A modified SAR protocol for optical dating of individual grains from young quartz samples. *Radiation Measurements* 42: 360–369, DOI 10.1016/j.radmeas.2006.12.016.

Ballarini M, Wintle AG and Wallinga J, 2006. Spatial variation of dose rate from beta sources as measured using single grains. *Ancient TL* 24: 1–8.

Bickel L, Luthgens C, Lomax J and Fiebig M, 2015. Luminescence dating of glaciofluvial deposits linked to the penultimate glaciation in the Eastern Alps. *Quaternary International* 357: 110–124, DOI 10.1016/j.quaint.2014.10.013.

Bøtter-Jensen L, Andersen CE, Duller GAT and Murray AS, 2003. Developments in radiation, stimulation and observation facilities in luminescence measurements. *Radiation Measurements* 37: 535–541, DOI 10.1016/S1350-4487(03)00020-9.

Buechi MW, Lowick SE and Anselmetti FS, 2017. Luminescence dating of glaciolacustrine silt in overdeepened basin fills beyond the last interglacial. *Quaternary Geochronology* 37: 55–67, DOI 10.1016/j.quageo.2016.09.009.

Bulur E, 2000. A simple transformation for converting CW-OSL curves to LM-OSL curves. *Radiation Measurements* 32: 141–145, DOI 10.1016/S1350-4487(99)00247-4.

Cunningham AC and Wallinga J, 2010. Selection of integration time-intervals for quartz OSL decay curves. *Quaternary Geochronology* 5: 657–666, DOI 10.1016/j.quageo.2010.08.004.

Duller GAT, 2006. Single grain optical dating of glacigenic deposits. *Quaternary Geochronology* 1: 296–304, DOI 10.1016/j.quageo.2006.05.018.

Duller GAT, Bøtter-Jensen L and Murray AS, 2000. Optical dating of single sand-sized grains of quartz: sources of variability. *Radiation Measurements* 32: 453–457, DOI 10.1016/S1350-4487(00)00055-X.

Duller GAT, 2003. Distinguishing quartz and feldspar in single grain luminescence measurements. *Radiation Measurements* 37: 161–165, DOI 10.1016/S1350-4487(02)00170-1.

Duller GAT, 2012. Improving the accuracy and precision of equivalent doses determined using the optically stimulated luminescence signal from single grains of quartz. *Radiation Measurements* 47: 770–777, DOI 10.1016/j.radmeas.2012.01.006.

Durcan JA, 2012. *Luminescence dating of sediments in Punjab, Pakistan: implications for the collapse of the Harappan Civilisation.* Aberystwyth University, UK.

Durcan JA and Duller GAT, 2011. The fast ratio: a rapid measure for testing the dominance of the fast component in the initial OSL signal from quartz. *Radiation Measurements* 46: 1065–1072, DOI 10.1016/j.radmeas.2011.07.016.

Feathers J, 2015. Luminescence dating at Diepkloof Rock Shelter – new dates from single-grain quartz. *Journal of Archaeological Science* 63: 164–174, DOI 10.1016/j.jas.2015.02.012.

Fu X, Li S-H and Li B, 2015. Optical dating of aeolian and fluvial sediments in north Tian Shan range, China: Luminescence characteristics and methodological aspects. *Quaternary Geochronology* 30: 161–167, DOI 10.1016/j.quageo.2015.03.001.

Fuchs M and Owen LA, 2008. Luminescence dating of glacial and associated sediments: review, recommendations and future directions. *Boreas* 37: 636–659, DOI 10.1111/j.1502-3885.2008.00052.x.

Gaar D, Lowick SE and Preusser F, 2014. Performance of different luminescence approaches for the dating of known-age glaciofluvial deposits from northern Switzerland. *Geochronometria* 41: 65–80, DOI 10.2478/s13386-013-0139-0.

Gaar D and Preusser F, 2012. Luminescence dating of mammoth remains from northern Switzerland. *Quaternary Geochronology* 10: 257–263, DOI 10.1016/j.quageo.2012.02.007.

Galbraith RF, Roberts RG, Laslett GM, Yoshida H and Olley JM, 1999. Optical dating of single and multiple grains of quartz from Jinmium rock shelter, northern Australia. Part I. Experimental design and statistical models. *Archaeometry* 41: 339–364, DOI 10.1111/j.1475-4754.1999.tb00987.x.

Godfrey-Smith D, Huntley D and Chen W, 1988. Optical dating studies of quartz and feldspar sediment extracts. *Quaternary Science Reviews* 7: 373–380, DOI 10.1016/0277-3791(88)90032-7.

Jacobs Z, Hayes EH, Roberts RG, Galbraith RF and Henshilwood CS, 2013. An improved OSL chronology for the Still Bay layers at Blombos Cave, South Africa: further tests of single-grain dating procedures and a re-evaluation of the timing of the Still Bay industry across southern Africa. *Journal of Archaeological Science* 40(1): 579–594, DOI 10.1016/j.jas.2012.06.037.

Jain M, Murray AS and Bøtter-Jensen L, 2003. Characterisation of blue-light stimulated luminescence components in different quartz samples: implications for dose measurement. *Radiation Measurements* 37: 441–449, DOI 10.1016/S1350-4487(03)00052-0.

Klasen N, Fiebig M, Preusser F, Reitner JM and Radtke U, 2007. Luminescence dating of proglacial sediments from the Eastern Alps. *Quaternary International* 164–165: 21–32, DOI 10.1016/j.quaint.2006.12.003.

Klasen N, 2008. *Lumineszenzdatierung glazifluvialer Sedimente im nördlichen Alpenvorland ("Luminescence dating of glaciofluvial sediments in the Northern Alpine Foreland")*. University of Cologne: 210 pp. (in German).

Klasen N, Fiebig M and Preusser F, 2016. Applying luminescence methodology to key sites of Alpine glaciations in Southern Germany. *Quaternary International* 420: 249–258, DOI 10.1016/j.quaint.2015.11.023.

Li B and Li S-H, 2006. Comparison of De estimates using the fast component and the medium component of quartz OSL. *Radiation Measurements* 41: 125–136, DOI 10.1016/j.radmeas.2005.06.037.

Lowick SE, Buechi MW, Gaar D, Graf HF and Preusser F, 2015. Luminescence dating of Middle Pleistocene proglacial deposits from northern Switzerland: methodological aspects and stratigraphical conclusions. *Boreas* 44: 459–482, DOI 10.1111/bor.12114.

McKeever SWS and Chen R, 1997. Luminescence models. *Radiation Measurements* 27: 625–661, DOI 10.1016/S1350-4487(97)00203-5.

Moska P and Murray AS, 2006. Stability of the quartz fast-component in insensitive samples. *Radiation Measurements* 41(7): 878–885, DOI 10.1016/j.radmeas.2006.06.005.

Murray AS and Wintle AG, 1999. Isothermal decay of optically stimulated luminescence in quartz. *Radiation Measurements* 30: 119–125, DOI 10.1016/S1350-4487(98)00097-3.

Murray AS and Wintle AG, 2000. Luminescence dating of quartz using an improved single-aliquot regenerative-dose protocol. *Radiation Measurements* 32: 57–73, DOI 10.1016/S1350-4487(99)00253-X.

Murray AS, Thomsen KJ, Masuda N, Buylaert JP and Jain M, 2012. Identifying well-bleached quartz using the different bleaching rates

of quartz and feldspar luminescence signals. *Radiation Measurements* 47: 688–695, DOI 10.1016/j.radmeas.2012.05.006.

Olley JM, Pietsch T and Roberts RG, 2004. Optical dating of Holocene sediments from a variety of geomorphic settings using single grains of quartz. *Geomorphology* 60: 337–358, DOI 10.1016/j.geomorph.2003.09.020.

Pietsch TJ, Olley JM and Nanson GC, 2008. Fluvial transport as a natural luminescence sensitiser of quartz. *Quaternary Geochronology* 3: 365–376, DOI 10.1016/j.quageo.2007.12.005.

Preusser F, Ramseyer K and Schlüchter C, 2006. Characterisation of low OSL intensity quartz from the New Zealand Alps. *Radiation Measurements* 41: 871–877, DOI 10.1016/j.radmeas.2006.04.019.

Preusser F, Blei A, Graf H and Schlüchter C, 2007. Luminescence dating of Würmian (Weichselian) proglacial sediments from Switzerland: methodological aspects and stratigraphical conclusions. *Boreas* 36: 130–142, DOI 10.1080/03009480600923378.

Rades EF, Fiebig M and Lüthgens C, in press. Luminescence dating of the Rissian type section in southern Germany as a base for correlation. *Quaternary International*.

Salcher BC, Starnberger R and Götz J, 2015. The last and penultimate glaciation in the North Alpine Foreland: New stratigraphical and chronological data from the Salzach glacier. *Quaternary International* 388: 218–231, DOI 10.1016/j.quaint.2015.09.076.

Schielein P, Schellmann G, Lomax J, Preusser F and Fiebig M, 2015. *Chronostratigraphy of the Hochterrassen in the lower Lech valley (Northern Alpine Foreland)*. E&G 64: 15–28.

Smith BW and Rhodes EJ, 1994. Charge movements in quartz and their relevance to optical dating. *Radiation Measurements* 23: 581–585, DOI 10.1016/1350-4487(94)90060-4.

Spencer J and Owen L, 2004. Optically stimulated luminescence dating of Late Quaternary glaciogenic sediments in the upper Hunza valley: validating the timing of glaciation and assessing dating methods. *Quaternary Science Reviews* 23: 175–191, DOI 10.1016/S0277-3791(03)00220-8.

Steffen D, Preusser F and Schlunegger F, 2009. OSL quartz age underestimation due to unstable signal components. *Quaternary Geochronology* 4: 353–362, DOI 10.1016/j.quageo.2009.05.015.

Thomsen KJ, Murray AS and Bøtter-Jensen L, 2005. Sources of variability in OSL dose measurements using single grains of quartz. *Radiation Measurements* 39: 47–61, DOI 10.1016/j.radmeas.2004.01.039.

Thomsen KJ, Murray AS and Jain M, 2012. The dose dependency of the overdispersion of quartz OSL single grain dose distributions. *Radiation Measurements* 47: 732–739, DOI 10.1016/j.radmeas.2012.02.015.

Thomsen KJ, Kook M, Murray AS, Jain M and Lapp T, 2015. Single-grain results from an EMCCD-based imaging system. *Radiation Measurements* 81: 185–191. DOI 10.1016/j.radmeas.2015.02.015.

Wallinga J, 2002. On the detection of OSL age overestimation using single-aliquot techniques. *Geochronometria* 21: 17–26.

Wintle AG and Murray AS, 2006. A review of quartz optically stimulated luminescence characteristics and their relevance in single-aliquot regeneration dating protocols. *Radiation Measurements* 41: 369–391, DOI 10.1016/j.radmeas.2005.11.001.